American Mineralogist, Volume 101, pages 222–230, 2016

SPECIAL COLLECTION: RATES AND DEPTHS OF MAGMA ASCENT ON EARTH

Timescales of magma storage and migration recorded by olivine crystals in basalts of the March-April 2010 eruption at Eyjafjallajökull volcano, Iceland

Marco Viccaro[1,*], Marisa Giuffrida[1], Eugenio Nicotra[1], and Renato Cristofolini[1]

[1]Università di Catania, Dipartimento di Scienze Biologiche, Geologiche e Ambientali, Sezione di Scienze della Terra, Corso Italia 57, I-95129, Catania, Italy

Abstract

The early eruptive phase of the 2010 eruption at the Fimmvörðuháls Pass, east of Eyjafjallajökull volcano, produced poorly evolved basalts with mildly alkaline affinity, and benmoreitic tephra were emitted during the second explosive phase from the summit vent of the volcano. In this study, textural features and chemical zoning preserved in olivine crystals of the early erupted basalts have been used to define the timescales of differentiation processes and magma ascent before the eruption. These lavas contain a mineral assemblage constituted by olivine ($Fo_{70–88}$) and plagioclase ($An_{57–83}$) in similar proportions with scarce clinopyroxene and opaque oxides. Olivine occurs as euhedral or embayed crystals characterized by different core compositions and zoning patterns. Three main olivine populations have been found, namely crystals with: (1) wide Fo_{88} cores with normal zoning toward narrow rims (P1); (2) ~Fo_{81} cores with either no zoning or slight reverse zoning patterns toward the rims (P2); (3) ~Fo_{77} cores with reverse zoning at the rims (P3). The olivine reverse zoning indicates that these poorly evolved magmas experienced mixing processes in addition to limited fractional crystallization at different levels of the plumbing system. Timescales of transfer dynamics before the eruption have been estimated through Fe-Mg diffusion modeling on these olivine populations. The olivine-melt equilibration through diffusion was triggered by interaction of magmas differing in their evolutionary degree. P1 and P2 crystals recorded a first event of interaction in a ~22 km deep reservoir that took place about one month before the emission of the analyzed products. Only part of P2 crystals records reverse zoning due to interaction with more basic magma bearing P1 crystals (which consequently develop normal zoning), suggesting fast timescales of magma mixing that prevented the complete homogenization. A second mixing event, which is evident in the P3 olivines, occurred at shallower levels (5–6 km of depth) ~15 days before the emplacement and can be considered the triggering mechanism leading to the eruption at the Fimmvörðuháls Pass. Integration of our timescales with seismic data relative to the hypocenter migration indicate rates of magma ascent throughout the deep plumbing system of ~0.01 m/s. This study provides evidence that magmas emitted at Eyjafjallajökull volcano, and more in general at similar other volcanic systems in ocean ridge settings, can undergo complex processes during their storage and transport in the crust, chiefly due to the presence of a multilevel plumbing system.

Keywords: Eyjafjallajökull, olivine, diffusion modeling, magma mixing, ascent dynamics

Introduction

Recent studies chiefly based on geophysical considerations have profoundly changed the view of a single-level, molten system of reservoirs distributed beneath the mid-ocean ridges (e.g., Dunn et al. 2000, and references therein). Mush zones constituted of liquid regions of variable dimensions and other portions characterized by various degrees of crystallization are thought more plausible to describe the physical configuration of magma storage zones beneath ocean ridges. The idea of a multilevel plumbing system, articulated through distinct paths of magma ascent, is more pronounced for important volcanic systems above ocean ridges characterized by central activity. The best examples of such kind are the Icelandic shield volcanoes (e.g., Katla, Eyjafjallajökull, Askja, Krafla, Grimsvötn, Bardarbunga). Magma transfer dynamics from the source zones up to the surface and eruption at these volcanic systems are not always easily understood, and requires that chemical and physical constraints are first made for the magma reservoirs (location, sizes, timescales of magmatic processes, etc.).

The presence of zoning in crystals is evidence for changes of the chemical and/or physical conditions of the magmatic system such as melt composition, oxygen fugacity, temperature, pressure, and volatile contents during their growth history (Wallace and Bergantz 2002, 2004, 2005; Ginibre et al. 2007; Streck 2008; Viccaro et al. 2010; Kahl et al. 2011, 2013). Furthermore, diffusion chronometry applied to compositionally zoned crystals has proved to be valuable for understanding either the reasons for or the timescales that lead to such changes (e.g., Zellmer et al. 1999; Costa et al. 2003, 2008; Costa and Chakraborty 2004; Costa and Morgan 2010; Morgan et al. 2004; Morgan and Blake

* E-mail: m.viccaro@unict.it

Special collection information can be found at http://www.minsocam.org/MSA/AmMin/special-collections.html.

2006; Kahl et al. 2011, 2013). As the crystals record physical and chemical changes of the magmatic environment, the intracrystalline diffusion starts and the chemical gradient among different zones of the crystal is reduced over time. The extent to which the zoning will be equilibrated by diffusion depends on many parameters such as the mineral structure, the elements involved in the process, temperature, and time. Thus, the zoning patterns preserved in minerals could be used to reconstruct the evolutionary processes that magmas underwent throughout the plumbing system and the duration of storage and transport in different environments, which together are among the most important goals of the modern volcanology.

In this study, the textural features and chemical zoning preserved in olivine crystals have been used to track the pre-eruptive history of basaltic magmas feeding the early phase of the 2010 eruption of Eyjafjallajökull volcano at the Fimmvörðuháls Pass. Estimations on timescales of magmatic processes acting beneath the Eyjafjallajökull volcano have been obtained by modeling the Fe-Mg diffusion observed in olivine chemical profiles. Our results provide elements to understand the nature and timing of magmatic processes before the eruption of primitive basalts in Iceland that, although infrequent, can present a significant hazard due to the limited timespan occurring between the beginning of magma ascent and the final magma extrusion.

The Eyjafjallajökull volcano

Geological setting and volcanism

Eyjafjallajökull volcano rises to a height of 1666 m at the southwestern end of the East Volcanic Zone (EVZ), which at present represents the most volcanically active region in Iceland (Fig. 1a). The EVZ is a propagating SW-NE trending rift located outside the main zone of spreading (the axial rift). This area includes 30 volcanic systems that, on the whole, account for ~79% of the total volume of erupted magmas in Iceland during the last 11 centuries. However, most of the emitted magma is accommodated by the active systems of Katla, Grimsvötn, Hekla, and Bardarbunga-Veidivötn (Fig. 1a; Thordarson and Larsen 2007). The EVZ is dominated by emission of tholeiitic magmas in its northeastern segment, whereas mildly alkaline magmas characterize the southwestern segment, which is currently propagating southwesterly (Thordarson and Larsen 2007 and references therein).

Eyjafjallajökull has been constructed through sub-glacial eruptions and its edifice is completely covered by an ice cap. Historic activity of Eyjafjallajökull has been characterized by long-lasting periods of quiescence, commonly interrupted by initial hydromagmatic explosions evolving to eruptive episodes with Strombolian to sub-Plinian styles. Prior to the 2010 A.D. eruption, the historical record includes a radial fissure eruption dated ~920 A.D. and two small-volume summit eruptions at 1612 A.D. and 1821–1823 A.D., which were identified through chrono-stratigraphic studies and analysis of historic chronicles (Thordarson and Larsen 2007; Dugmore et al. 2013 and references therein). Extensive intrusions at 4.5 and 6.5 km of depth, with estimated volumes of $10–17 \times 10^6$ m^3 and $21–31 \times 10^6$ m^3, respectively, occurred beneath the Eyjafjallajökull volcano in 1994 and 1999, as revealed by InSAR observations, GPS geodetic measurements, and optical tilt leveling (Pedersen and Sigmundsson 2004, 2006; Sturkell et al. 2003; Sigmundsson et al. 2010).

All the historic eruptions of Eyjafjallajökull were more or less contemporaneous with eruptions or evidence of magma movements [i.e., glacier floods and several small earthquakes] at the nearby Katla volcano (~25 km to the east). This trend held during the 2010 eruption at Eyjafjallajökull, as demonstrated by several seismic swarms beneath Katla in the 2011–2012 period. Sturkell et al. (2003) also argued that magma movements took place at shallow levels beneath Katla in 1999 at the same time of a magma intrusion beneath Eyjafjallajökull, both evidenced by GPS and seismic data.

The March-May 2010 eruption

The 2010 event at Eyjafjallajökull volcano was characterized by two distinct eruptive phases: an initial effusive flank eruption, characterized primarily by eruption of lava flows at the Fimmvörðuháls Pass (Fig. 1b), and a second explosive summit eruption producing ash-tephra fall-out that had heavy impact

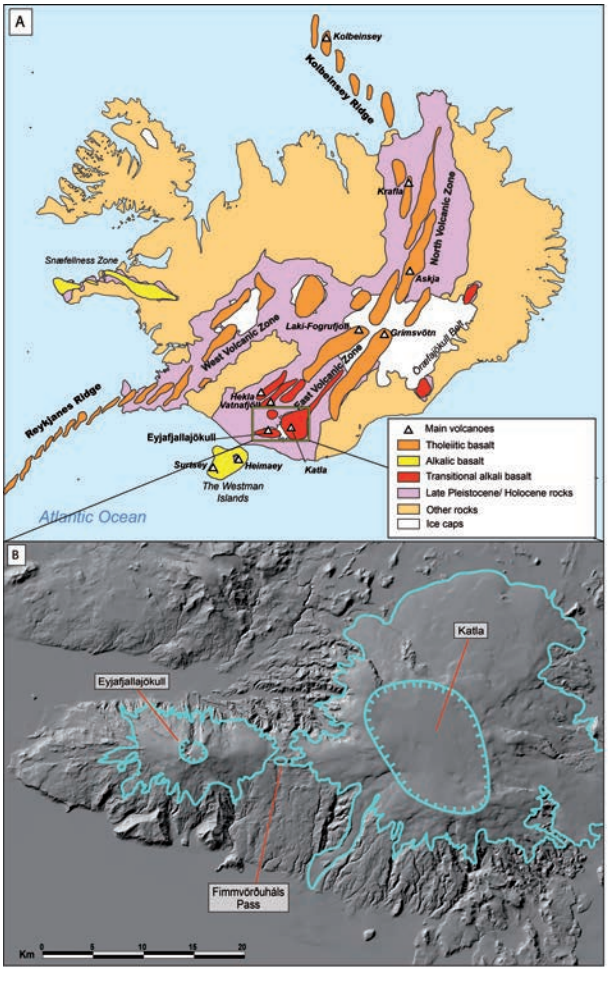

Figure 1. (**a**) Schematic map of Iceland with composition of the volcanic rocks belonging to different neo-volcanic zones. (**b**) Digital Elevation Model of the Eyjafjallajökull and Katla volcanoes and the area of Fimmvörðuháls Pass (source: National Land Survey of Iceland, http://www.lmi.is/en/okeypis-kort/). (Color online.)

on air-traffic in a large part of Europe. Three months of intense seismicity and deformation preceded the onset of the flank eruption on March 20, 2010 (Gudmundsson et al. 2010; Sigmundsson et al. 2010; Sigmarsson et al. 2011, and references therein). Over the previous 18 yr, several signals of volcanic unrest were detected through geodetic and geophysical investigations, such as earthquakes and flank deformation attributed to magma injections beneath the volcano. Precursory signals, recorded since late December 2009, were the prelude of the opening on March 20, 2010, of a ~300 m long fissure at Fimmvörðuháls Pass, between the Eyjafjallajökull and the Myrdalsjökull glaciers (Figs. 1b and 2). The eruption produced lava fountains up to 150 m high and limited tephra fallout. On March 31, a new fissure opened with an angle of 50° from that of March 20 (trending N15°W), where on April 2 the eruptive activity moved. The activity produced a northward expanding small a'a lava flow field, filling deep gullies excavated on the flanks of the Eyjafjallajökull volcano and forming spectacular lava falls (Fig. 2). Effusions from these fissures continued until April 12, with an average magma emission rate of ~13 m^3/s (Sigmundsson et al. 2010). This led to the formation of two small scoria cones at the active vents and a lava field of basalts with mildly alkaline affinity (Sigmarsson et al. 2011; Keiding and Sigmarsson 2012; Moune et al. 2012). At the end of the flank eruption, the estimated total volume of emitted magma was approximately 25×10^6 m^3 (Sigmundsson et al. 2010 and references therein).

After just two days of rest, the volcanic activity started again in the early morning of April 14 at the central crater of Eyjafjallajökull volcano, preceded by a seismic swarm with hypocenters fast moving from 7 km depth toward the ice-capped summit of the volcano (Tarasewicz et al. 2012). The magma-ice interaction gave rise during the first days to a hydromagmatic, highly explosive central eruption that produced a ~10 km high ash plume (Sigmundsson et al. 2010 and references therein; Sigmarsson et al. 2011). Thereafter, the hydromagmatic activity decreased and evolved to purely magmatic after less than one week. Main peaks of the explosive activity were recorded at the onset of the summit eruption and later on 5–6 May, with emission rates on the order of 10^6 kg/s (Sigmarsson et al. 2011). The sustained magma discharge continued until May 22 with emission of fine ash and dust with benmoreitic-trachytic composition.

Sampling and analytical methods

A total of 16 volcanic rock samples was collected from the last-emitted products of the lava flow field developed between March 20 and April 12, 2010, during the eruption at Fimmvörðuháls Pass, east of the summit of Eyjafjallajökull volcano (Figs. 1b and 2). Samples are from the activity of April 10–12, just before the end of the eruption. Polished thin sections have been made for petrographic and textural analysis of olivine crystals as well as for in situ microanalysis. High-contrast backscattered electron (BSE) images, elemental X-ray maps, and microanalytical data were obtained at the Dipartimento di Scienze Biologiche, Geologiche e Ambientali of Catania, Italy, on ~50 selected olivine crystals representative of the identified dimensional classes and textures using a Tescan Vega-LMU scanning electron microscope equipped with an EDAX Neptune XM4-60 energy-dispersive system, which is characterized by an ultra-thin Be window, coupled with an EDAX wavelength-dispersive low-energy X-ray spectrometer (WDS LEXS) calibrated for light elements. Operating conditions were set at 20 kV accelerating voltage and ~8 nA beam current for obtaining high-contrast BSE images. At the same operating conditions, elemental X-ray maps have been acquired with dwell time of 500 µs for

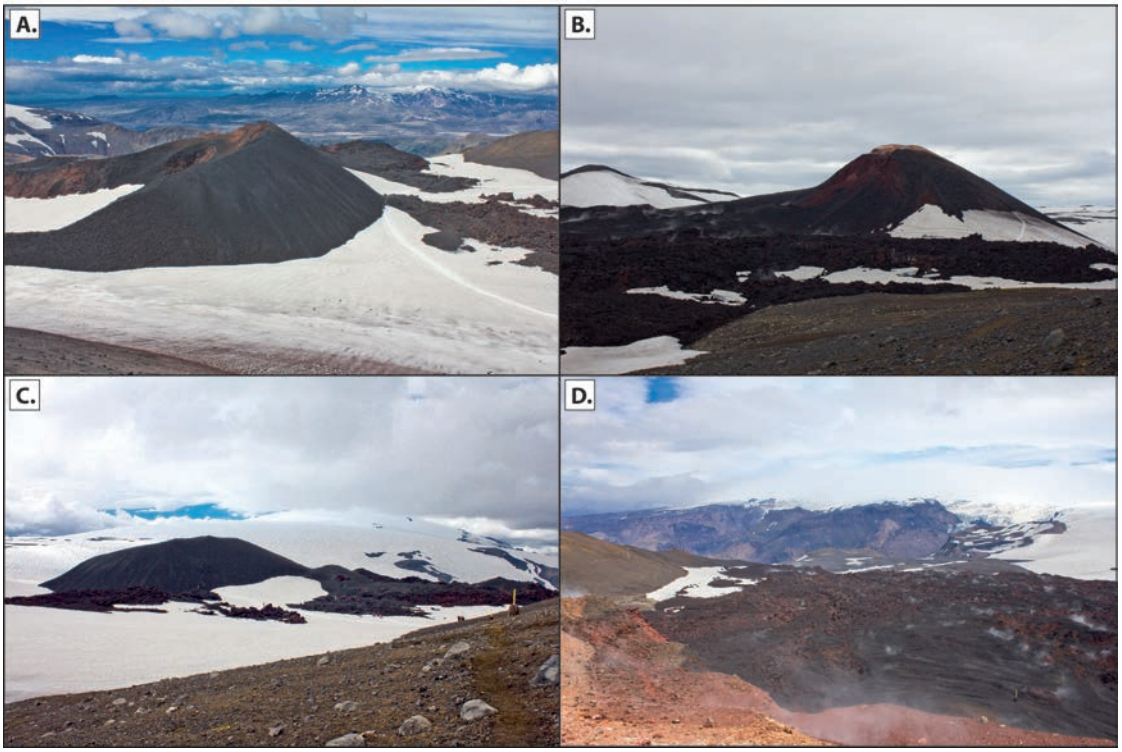

Figure 2. (**a** and **b**) Scoria cones and a'a lava flow field at Fimmvörðuháls Pass. (**c**) Part of the lava flow field at the Fimmvörðuháls Pass with top of the Eyjafjallajökull volcano on the background. (**d**) Lava flow field at the Fimmvörðuháls Pass with the Myrdalsjökull glacier on the background. (Color online.)

128 frames (total time for acquisition of each X-ray map around 4.5 h). Operating conditions for the analysis of major element abundances in olivine and the other mineral phases were set at 20 kV accelerating voltage and 0.2 nA beam current. Repeated analyses on internationally certified Fo-rich olivine and glass internal standards during the analytical runs ensure precision for all the collected elements on the order of 3–5% (all data available in deposit[1]).

Characteristics of the volcanic rocks

Petrography and chemistry of minerals

Volcanic products erupted during the first phase of the 2010 eruption at Eyjafjallajökull are basalts (Sigmarsson et al. 2011; Keiding and Sigmarsson 2012; Moune et al. 2012) with homogeneous petrographic features. Differences are mainly related to groundmass textures and the modal abundance of mineral phases. Samples are mildly porphyritic (15 to 20 vol% of phenocrysts) and highly vesiculated; phenocrysts mostly consist of plagioclase and olivine in similar proportions, together making up 80–85 vol% of the total phenocryst content (Fig. 3a). The mineral assemblage also includes scarce clinopyroxene (~10–15 vol%) and opaque oxides (<5 vol%). Phenocrysts generally occur as single crystals with variable grain sizes. Glomerophyric structures involving olivine, plagioclase, and clinopyroxene are also present. The groundmass is vitrophyric to hyalopilitic with plagioclase microlites as the predominant phase (Fig. 3a).

Plagioclase crystals vary in size from large crystals (up to 2400 μm) to micro-phenocrysts (~200 μm) with labradorite (An_{53}) to bytownite (An_{83}) compositions (Fig. 3a; Supplementary Table 1[1]). The medium-size (500–1500 μm) plagioclase generally occurs as euhedral crystals, tabular in shape and homogeneous in composition. Analyses under the polarized light microscope do not reveal significant optical zoning. Also skeletal, swallow-tailed microlites are present in the analyzed sections. The largest grains commonly exhibit a coarsely sieved core, embedded by oscillatory-zoned outer rims. Phenocrysts affected by extensive dissolution (rounded edges) or with sieve-textures at the rim have been also found.

Olivines are present as large euhedral to anhedral phenocrysts up to ~4.5 mm in size (Figs. 3a–3d). Most of the largest grains are strongly destabilized with extensive embayments that extend deeply into the crystal core; these embayments do not show reaction rims. Smaller crystals (from ~200 to 600 μm) are generally euhedral, though some of them have slight embayed morphology. Olivine core compositions vary from Fo_{88} to Fo_{77} (see Supplementary Table 1[1]). In this regard, rim-to-rim major element profiles allowed three main crystal populations to be identified. Details of textural features and zoning patterns of the three populations are described in the following section.

Clinopyroxenes mostly occur as small euhedral phenocrysts ranging in size from 200 to 600 μm, rarely found as large single crystals (up to 1200 μm in size) or in aggregates with plagioclase and olivine. Their compositions are in the range Wo_{38-45}, En_{40-51}, Fs_{12-16} (see Supplementary Table 1[1]).

Two opaque oxides have been identified with compositions either of titaniferous-magnetite or Cr-spinel (Supplementary Table 1[1]). The former is from subhedral to euhedral, with sizes up to few tens of micrometers, whereas the latter commonly

[1] Deposit item AM-16-15365, Electronic Supplementary Material. Deposit items are free to all readers and found on the MSA web site, via the specific issue's Table of Contents (go to http://www.minsocam.org/MSA/AmMin/TOC/).

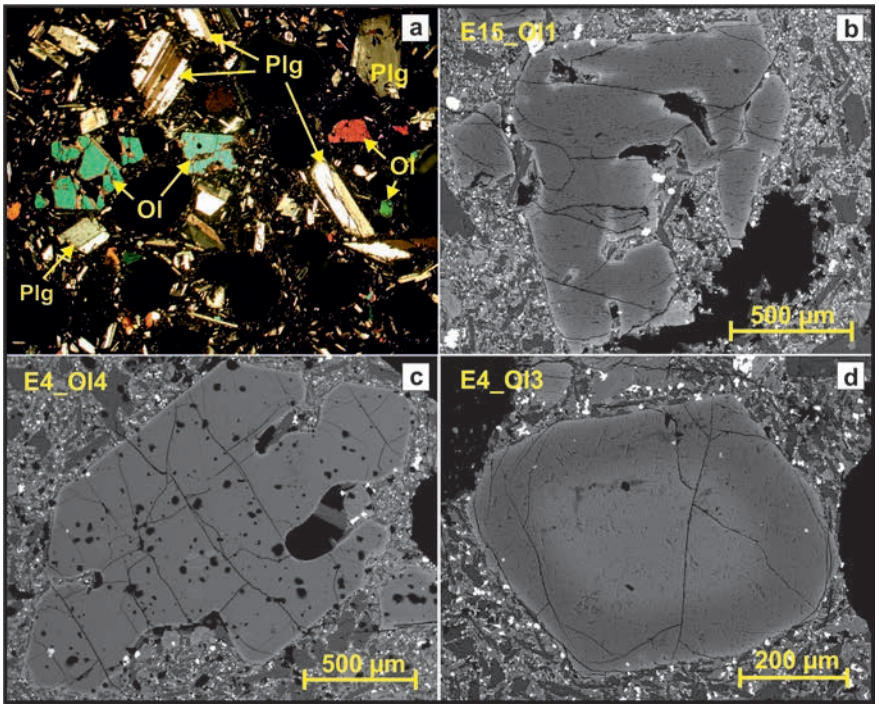

Figure 3. (**a**) Photo taken under the polarized light microscope (crossed Nicols) showing the petrographic features of a representative basalt emitted during the 2010 eruption at the Fimmvörðuháls Pass. (**b**, **c**, **d**) BSE images taken at the scanning electron microscope of representative P1, P2, and P3 olivine crystals, respectively. (Color online.)

occurs as anhedral crystals, up to 200 µm in size, enclosed in the largest olivine crystals with Fo_{88} and Fo_{81}.

Textural and compositional features of olivine crystals

Major element analyses were performed along rim-to-rim profiles on olivine crystals with sizes ranging from ~400 to 2500 µm. Traverses crosscut the center of the crystal, with step of 7–13 µm between each analyzed spot. Three main olivine populations have been identified on the basis on their core compositions, namely: (1) the first population (P1) refers to olivine with Fo_{88} cores (Fig. 3b); (2) the second population (P2) pertains to olivine with ~Fo_{81} cores (Fig. 3c); (3) the third population (P3) is constituted by olivine cores at ~Fo_{77} (Fig. 3d; Supplementary Table 1[1]).

The P1 olivines (~Fo_{88}) are resorbed with extensive embayments (Fig. 4). They are uncommon (2–3 individuals per thin section) and typical of the largest phenocryst (900–2500 µm across). P1 olivines display nearly flat compositional profiles at their wide cores and normally zoned rims, decreasing to Fo_{70} at the outermost rim (50–80 µm).

Olivines belonging to P2 and P3 include euhedral or embayed large crystals with size ranging from 900 to 1500 µm or smaller olivines (~600 µm). P2 crystals constitute the most abundant population, being ~70% of the olivine phenocrysts observed in the analyzed rocks (Fig. 5). These olivines show two distinct zoning patterns: (1) constant ~Fo_{81} core composition and normally zoned rims, which is the dominant zoning pattern in P2; (2) reverse zoning with slightly increasing Fo toward the rim (up to ~Fo_{83}), which occurs less commonly than normal zoning. Independently from the zoning pattern type, all the P2 crystals record a sudden drop to Fo_{73} in the outermost envelopes (last 30–50 µm).

All the P3 olivine crystals have core compositions at ~Fo_{77} with a marked reversely zoning toward the rims (Fig. 6). Variable ΔFo in the reverse zoned portion of crystals leads to define two sub-populations: P3a) with minor variations (~ΔFo_5), shifting the rim composition from ~Fo_{77} to ~Fo_{82}; P3b) with slightly more consistent changes (~ΔFo_8) that produce ~Fo_{85} envelopes. The outermost rims are normally zoned with decreasing Fo content to ~Fo_{70}.

Storage zones and processes

Compositional differences of the three populations of olivine crystals, which were found in the volcanic rocks emitted at the Fimmvörðuháls Pass during the 2010 eruption, necessarily imply the presence of three different magmatic environments characterized by changes of one or more of the above mentioned chemical-physical parameters. Various studies of Fe-Mg partitioning between olivine and basaltic liquids showed that the $^{Ol/Liq}K_{DFe\text{-}Mg}$ varies little with temperature and melt composition, being constant at 0.30 under pressures <2–3 GPa (Roeder and Emslie 1970). Conversely, the pressure dependence of $^{Ol/Liq}K_{DFe\text{-}Mg}$ is more marked, in a way that it is positively correlated with pressure (Herzberg and O'Hara 1998; Putirka 2005; Toplis 2005). This means that olivines crystallizing from liquids similar in their temperature and composition evolve to lower Fo contents under decreasing pressure.

The physical and chemical conditions of crystallization for the three olivine populations have been constrained through two-step thermodynamic modeling using the MELTS code (Ghiorso and Sack 1995; Asimow and Ghiorso 1998). A mantle-equilibrated

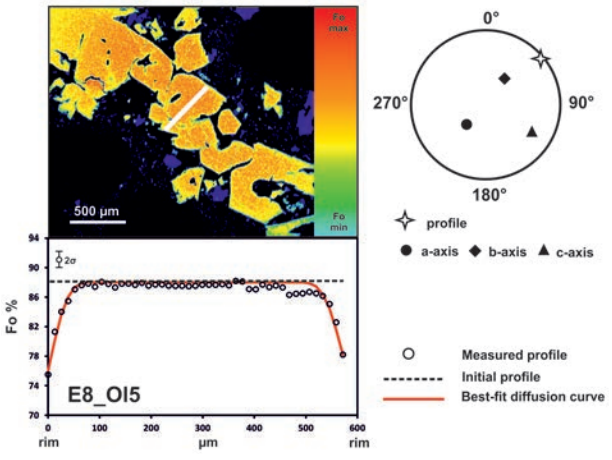

Figure 4. X-ray map for Mg, rim-to-rim zoning profile (white line on the X-ray map) and Fe-Mg diffusion modeling for a representative P1 olivine crystal, with ~Fo_{88} core and normal zoning at the rim, found in the basalts emitted at the Fimmvörðuháls Pass during the 2010 eruption. The figure shows the rim-to-rim profile for the forsterite concentration (Fo%) measured on the E8_Ol5 olivine (circles). The black dashed line indicates the initial concentration profile prior to the diffusion, whereas the red line reveals the best-fit diffusion model for the observed zoning profile. The stereographic plot indicates the angular relations between the *a*, *b*, and *c* crystallographic axes in olivine and the directions of the measured rim-to-rim traverse. (Color online.)

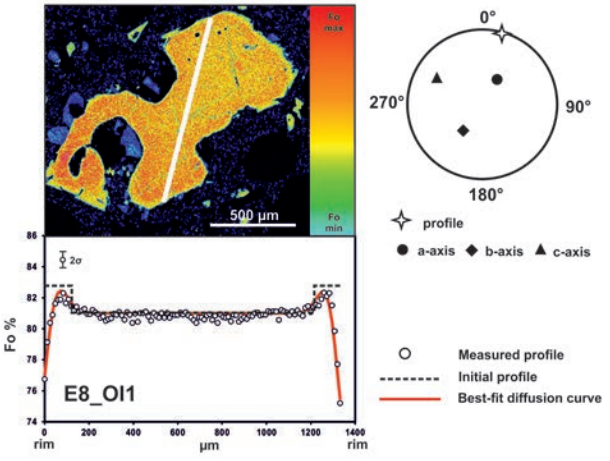

Figure 5. X-ray map for Mg, rim-to-rim zoning profile (white line on the X-ray map) and Fe-Mg diffusion modeling for a representative P2 olivine crystal, with ~Fo_{81} core and reverse zoning at the rim, found in the basalts emitted at the Fimmvörðuháls Pass during the 2010 eruption. The figure shows the rim-to-rim profile for the forsterite concentration (Fo%) measured on the E8_Ol1 olivine (circles). The black dashed line indicates the initial concentration profile prior to the diffusion, whereas the red line reveals the best-fit diffusion model for the observed zoning profile. The stereographic plot indicates the angular relations between the *a*, *b*, and *c* crystallographic axes in olivine and the directions of the measured rim-to-rim traverse. (Color online.)

composition of the 2010 Eyjafjallajökull lavas has been chosen as the starting liquid and considered the parental liquid for all the three populations, even though we have evidence for open-system processes (i.e., magma mixing). However, mixing occurred between magmas similar in their compositions, which means that errors deriving from the use of a single, evolving composition through fractional crystallization modeled by MELTS are restricted. Effects due to the limited fractionation of these magmas have been removed by adding ~10–15% of Fo_{88} olivine until the calculated liquid has the crystallizing olivine with Fo_{88}, representative of equilibrium with a primary magma at mantle conditions (P1 olivines). In the first step of simulation, we have tried to reproduce the physical-chemical conditions of crystallization for the P2 olivines (~Fo_{81}) using the range of physical-chemical parameters defined through geothermobarometry by Keiding and Sigmarsson (2012) for the crystallization of these basalts, i.e., pressure between 600 and 650 MPa, temperature between 1161 and 1174 °C, H_2O between 0.5 and 0.9 wt%. For this reason, parameters have been set as follows for the first step of simulation: pressure between 630 and 600 MPa (representative of crystallization at 24–23 km of depth for a crust density of 2.8 g/cm^3; cf. Tarasewicz et al. 2012), temperature between 1180 and 1160 °C, H_2O = 0.7 wt%. Several attempts (n >100) have been done, crossing the above-defined X-P-T parameters. However, P2 olivines (~Fo_{81}), coexisting with orthopyroxene and clinopyroxene of augitic composition, starts to crystallize at pressure of 615 MPa only if temperature is raised at 1210 °C and f_{O_2} fixed at the NNO buffer (~3.5×10^{-3} Pa). Lower temperatures or more oxidizing redox conditions do not allow crystallization of P2 olivines and the associated paragenesis. Assuming that more fayalitic olivines (such as P3 olivines at ~Fo_{77}) are produced through crystallization from a slightly more evolved liquid and/or at different physical conditions, there is needing of a further simulation at changed chemical-physical conditions. The final liquid resulting from the first step of simulation has been used as starting liquid in the second step. Even in this case, several attempts (n > 100) have been done, crossing various X-P-T conditions. The crystallization of ~Fo_{77} olivines from the starting liquid composition can be reproduced only decreasing pressure and temperature at more oxidizing redox conditions and slightly higher water contents. For the second step of simulation, parameters have been therefore set as follows: pressure between 170 and 120 MPa (representative of crystallization at 6–4.5 km of depth for a crust density of 2.8 g/cm^3; cf. Tarasewicz et al. 2012), temperature between 1200–1140 °C, f_{O_2} at the QFM buffer and H_2O = 0.9 wt% (cf. Keiding and Sigmarsson 2012). Under these conditions, P3 olivines (~Fo_{77}) starts to crystallize at pressure of 145 MPa, temperature of 1150 °C, and f_{O_2} ~1.7×10^{-4} Pa.

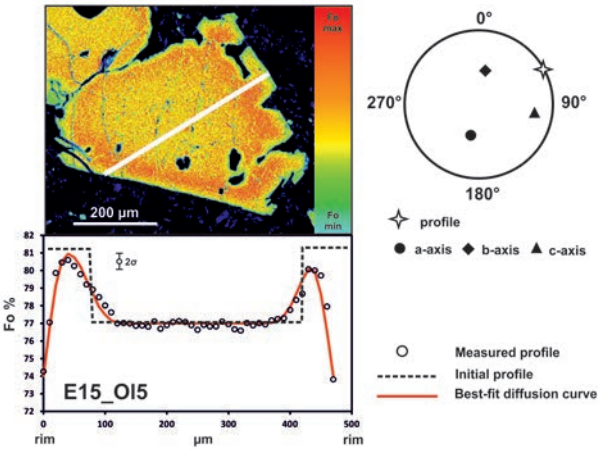

FIGURE 6. X-ray map for Mg, rim-to-rim zoning profile (white line on the X-ray map) and Fe-Mg diffusion modeling for a representative P1 olivine crystal, with ~Fo_{77} core and marked reverse zoning at the rim, found in the basalts emitted at the Fimmvörðuháls Pass during the 2010 eruption. The figure shows the rim-to-rim profile for the forsterite concentration (Fo%) measured on the E15_Ol5 olivine (circles). The black dashed line indicates the initial concentration profile prior to the diffusion, whereas the red line reveals the best-fit diffusion model for the observed zoning profile. The stereographic plot indicates the angular relations between the a, b, and c crystallographic axes in olivine and the directions of the measured rim-to-rim traverse. (Color online.)

The cores of the three olivine populations are flat, i.e., they do not present any compositional zoning over widths of hundreds of micrometers. This behavior could reflect residence for significant periods of time at high temperature, allowing complete equilibration through Fe-Mg diffusion prior to the rim overgrowth. Indeed, different zoning features at the rim of the three populations indicate different magmatic histories before the eruption. P1 olivines show peculiar features, as they are namely: (1) resorbed with extensive embayments; (2) scarce (2–3 crystals per thin section); (3) typical of the largest phenocrysts (900–2500 µm); (4) the most magnesian (Fo_{88}) of the entire data set; (5) with nearly constant core compositions and normally zoned rims (Fig. 4). The core characteristics are typical of unperturbed growth from a melt (hereafter called M1) almost equilibrated with the mantle. The presence of these crystals suggests that pre-eruptive dynamics have been influenced in some way by the ascent of the M1 magma from the source zones.

P2 olivines (~Fo_{81}) with normal zoning are the most abundant (~70%) in the emitted products. Their crystallization occurred from a magma (hereafter called M2) slightly more evolved than M1. The subordinate reversely zoned envelopes in some P2 olivines (up to ~Fo_{83}) reflect interaction with a magma necessarily more basic, whose olivine crystallizing at equilibrium is more forsteritic than Fo_{83} (Fig. 5). The Fo decrease at the rim of P1 olivines coupled with Fo increase around P2 crystal cores suggest that the mixing process involved M1 and part of M2 in the magma reservoir at the mantle-crust boundary, which is located at ~22 km b.s.l. beneath the Eyjafjallajökull volcano (Tarasewicz et al. 2012 and references therein; Fig. 7). Such deep magma reservoirs are usually present underneath central volcanoes in different areas of Iceland, especially in relation to the most active portions of the rift branches (Searle 2013 and references therein). Although the precise size of this reservoir beneath Eyjafjallajökull is not known, its bottom and top have been constrained, respectively, at depths of 24 and 21 km on the grounds of the location of the micro-earthquake foci occurred between March 6 and May 31, 2010 (Tarasewicz et al. 2012; Fig. 7). The result of mixing between M1 and M2 is a hybrid magma (hereafter called M3; Fig. 7), which carried during its ascent the P1 and P2 olivines. We infer that the mixing process within the deep reservoir had very fast timescales because most of

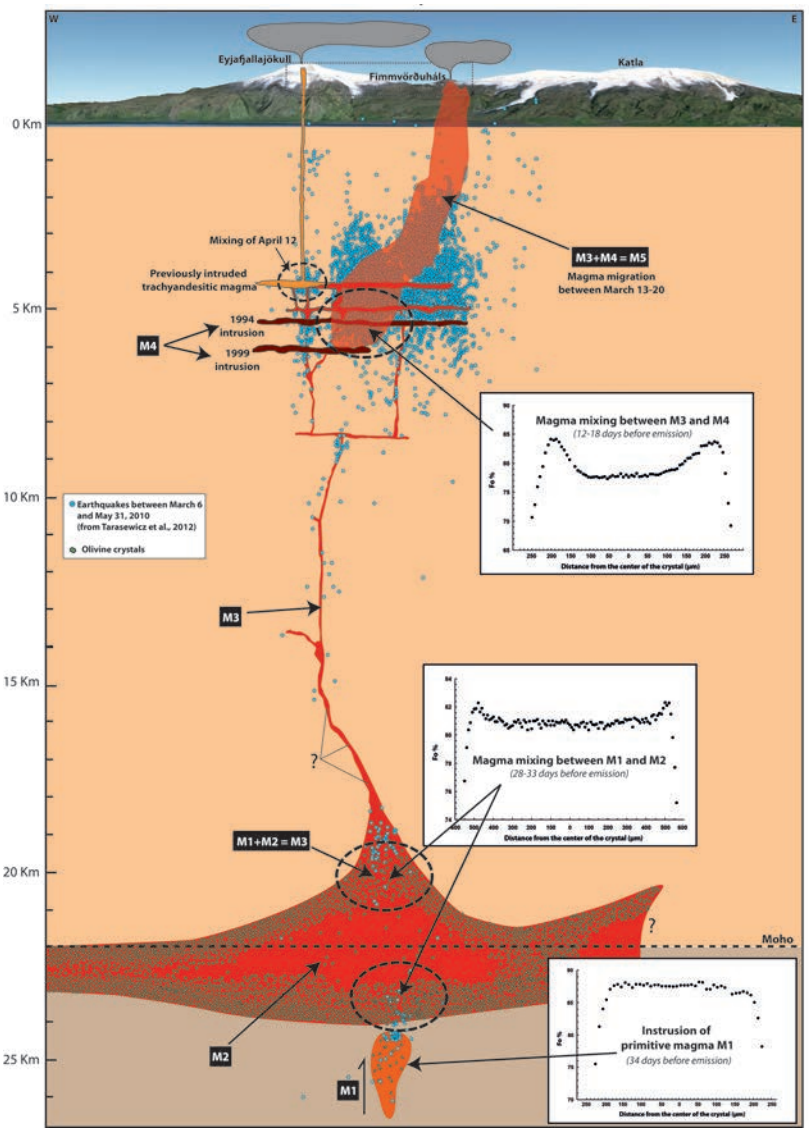

FIGURE 7. Cartoon of the petrological evolution leading to the 2010 eruption at the Fimmvörðuháls Pass and at the summit of Eyjafjallajökull volcano. Moho discontinuity is reported at ca. 22 km b.s.l. (cf. Tarasewicz et al. 2012 and references therein). Blue dots represent the locations of earthquake hypocenters during the period March 6 to May 31, 2010. The magmatic history starts with ascent from the mantle of the primitive magma (M1) carrying P1 olivines (with Fo_{88} cores). Considering that the analyzed products have been erupted between April 10 and 12, 2010, the diffusion modeling of P1 olivines dates a first event of intrusion of M1 into a deep magma environment ~34 days before the emission that coincide with the first detected earthquakes at 23–26 km of depth. At this depth, M1 magma mixed with the residing slightly more evolved magma (M2) that bears P2 olivines (with Fo_{81} cores). Mixing between M1 and M2 produced a new magma (M3), as testified by reverse Fo zoning (up to Fo_{83}) in some P2 crystals. Diffusion modeling dates this mixing event between 28 and 33 days before the emission on April 10–12, 2010. M3 magma started its ascent carrying P1 and P2 olivines and mixed at 4.5–6 km b.s.l. with a residing magma (M4) already intruded during 1994 and 1999 (Pedersen and Sigmundsson 2004, 2006; Sturkell et al. 2003; Sigmundsson et al. 2010) that bears P3 olivines (with Fo_{77} cores). This mixing event, testified by reverse Fo zoning ($Fo_{82–85}$) in P3 olivines, is dated by diffusion modeling between 12 and 18 days before the emission of the April 10–12 lavas. Result of this second mixing event is the final hybrid magma that intruded through an E-W-oriented dike and was erupted at the Fimmvörðuháls Pass (M5) between March 20 and April 12, 2010. The trachyandesitic magma reservoir that mixed with less differentiated magma on April 12 (Sigmarsson et al. 2011) is reported in the figure. (Color online.)

the P2 olivines did not register any reverse zoning. This feature could be attributed to lack of complete homogenization of the magma volume involved in the mixing process probably due to the rapid magma ascent toward the surface. This prevented the development of compositional changes in part of the crystals.

Compositional zoning data support the occurrence of a second mixing event at shallower depth. End-members of this second interaction could be M3 and a more evolved magma stored in the crust (hereafter called M4), as suggested by the more fayalitic core compositions of P3 olivine crystals (~Fo_{77}) with respect to P1 and P2 (Fig. 6). Magma mixing is markedly evident at the rim of P3 olivines, with Fo contents growing from Fo_{77} at the cores to Fo_{82}-Fo_{85} toward the rims (Fig. 6). The presence of the inferred M4 reservoir is supported by InSAR observations, GPS geodetic measurements, and optical tilt leveling data by several authors, who provide evidence of two 4.5 and 6.5 km deep intrusions beneath the Eyjafjallajökull volcano that took place in 1994 and 1999, respectively (Fig. 7; Pedersen and Sigmundsson 2004, 2006; Sturkell et al. 2003; Sigmundsson et al. 2010). In the next section, time constraints to the above mentioned magma dynamics are provided.

TIMESCALES OF MAGMA RECHARGE AND TRANSFER

To assess timescales of intrusion and open system processes such us magma mixing events before the 2010 Eyjafjallajökull flank eruption, the approach of Costa et al. (2008) and Costa and Morgan (2010) was adopted to model the diffusion-controlled re-equilibration of the Fe-Mg zoning of olivine. In numerical implementations, concentrations are described as a function of space (x) and time (t) and are directly related to values of the diffusion coefficients (D) along the measured profile. Thus, time evolution of the initial concentration distribution of the crystal can be traced until a new profile that fit the observed concentration profile is obtained. Due to the strong diffusion anisotropy, crystals were preliminarily selected to minimize uncertainties on time determination related to the section orientation with respect to the fast diffusion direction (c-axis), following the selection criteria listed in Costa and Chakraborty (2004) and Shea et al. (2015). The modeling has been performed by using Fick's Law-based diffusion equations with concentration dependent diffusion

coefficients ($D_{Fe\text{-}Mg}$); we assumed the measured concentration at the rim of the crystals as boundary conditions (see Supplementary Table 2[1]). The expression for calculating the Fe-Mg diffusion coefficients along [001] is from Dohmen and Chakraborty (2007). Coefficients were calculated at T = 1210 °C, P = 615 MPa, and f_{O_2} at ~3.5×10^{-3} Pa for the P1 and P2 populations, and at T = 1150 °C, P = 145 MPa, and f_{O_2} at ~1.7×10^{-4} Pa for the less forsteritic P3 crystals (Table 1). Such parameters have been chosen in accordance with the initial T, P, and f_{O_2} values of crystallization derived through our MELTS simulations, and are also consistent with the range of crystallization conditions defined for the early basaltic products of the 2010 eruption and the depths of magma storage beneath the volcano as described above (cf. Keiding and Sigmarsson 2012; Tarasewicz et al. 2012 and references therein). Anisotropy-corrected diffusivity along the direction of the profile (D*trav*) was obtained taking into account how the compositional traverses were oriented with respect to the olivine crystallographic *a*, *b*, and *c* axes (respectively coinciding with the optical indicatrix axes X, Y, and Z measured by conoscopic observations under a polarizing optical microscope equipped with a Zeiss 4 axis universal stage) to further improve the accuracy and precision on time calculations (cf. Costa and Chakraborty 2004; Shea et al. 2015). After application of all the correction criteria (i.e., influence of sectioning, diffusion anisotropy, crystal morphology), the model replicates diffusion times with a high degree of precision, although the number crystals suitable for calculation is considerably reduced (Table 1; deposit[1]). Uncertainties are mainly related to the temperature and oxygen fugacity determination. A temperature uncertainty of ±10 °C yields errors of 1 day (2σ) on the timescale estimates; f_{O_2} variation of one order magnitude produces errors of ca. 3 days (2σ). Conversely, the pressure dependence is small, with time oscillations of ca. 1 h for pressure changes of 10 MPa, at constant temperature and f_{O_2}.The chemical records preserved in olivine cores of the basalts erupted at Fimmvörðuháls Pass are evidence of at least three compositionally distinct magmatic environments where crystals grew close to equilibrium. Later, at the rims, they developed chemical gradients as a consequence of changed conditions. Awareness of the magmatic process causing disequilibrium in olivines is important to set the initial composition before re-equilibration of the system through diffusion. The high and constant Fo content at the P1 crystal core implies an early growth stage in a primitive host magma under unperturbed chemical and physical conditions. The decreased Fo content at the rims of the P1 crystals has been attributed to interactions with more evolved magmas during the intrusion at crustal levels, to achieve the new chemical and physical equilibrium at lower Fo. Therefore, through the Fe-Mg diffusion model we tried to estimate the timescale of this early intrusion and mixing at crustal depth (Fig. 4). The presence of at least two magma storage zones beneath Eyjafjallajökull volcano has been recognized through the zoning patterns preserved in the P2 and P3 olivine crystals (Figs. 5 and 6). Indeed, the core compositions at Fo_{81} (P2) and Fo_{77} (P3) suggest their growth in different magma environments, from melts more evolved than that of the P1 crystals. Reverse Fo zoning at the rim of both populations reflects mixing consequent to mafic recharge. These two recharging events produced chemical gradients at the crystal rims, and are considered responsible for triggering diffusion. Modeling of the chemical zoning in P2 and P3 olivines leads then to define timing of these mixing events (Figs. 5 and 6).

Table 1. Calculated timescales of re-equilibration and main parameters used for modeling the Fe-Mg diffusion of selected olivine crystals from the 2010 basaltic eruption at Eyjafjallajökull

Population	Olivine	Core comp. (Fo %)	T (°C)	P (kbars)	f_{O_2} (Pa)	D*trav* (μm²/s)	Avg. time (days)
P1	E8_Ol5	88	1210	6.15	3.55×10^{-4}	1.31×10^{-4}	34
P2	E4_Ol2	81	1210	6.15	3.55×10^{-5}	4.61×10^{-4}	33
P2	E8_Ol1	81	1210	6.15	3.55×10^{-5}	2.94×10^{-4}	28
P3	E4_Ol5	77	1150	1.45	2.19×10^{-5}	1.05×10^{-4}	18
P3	E15_Ol5	77	1150	1.45	2.19×10^{-5}	1.63×10^{-4}	18
P3	E15_Ol7	77	1150	1.45	2.19×10^{-5}	2.95×10^{-4}	12
P3	E3_Ol1	78	1150	1.45	2.19×10^{-5}	2.35×10^{-4}	18
P3	E15_Ol6	78	1150	1.45	2.19×10^{-5}	1.00×10^{-4}	16
P3	E8_Ol4	79	1150	1.45	2.19×10^{-5}	1.05×10^{-4}	12

Based on our calculations, the chemical zoning of P1 crystals requires ~34 days to re-equilibrate through diffusion; this result matches well the timescale obtained for the diffusion event in P2 crystals (30 days on average), suggesting an interaction between the P1 and P2 host magmas about one month before the emission of the analyzed products on April 10–12 (Figs. 4 and 5; Table 1). The micro-earthquake locations provided by Tarasewicz et al. (2012) confirm that a magma intrusion occurred at 21–24 km of depth about one month before the 2010 flank eruption at Eyjafjallajökull (Fig. 7). The more-evolved P3 olivines record timescales of re-equilibration that are significantly shorter than those obtained for P1 and P2 crystals (Fig. 6). Time estimations indicate that the second mixing event recorded by rims of the P3 olivines occurred about two weeks before magma emission at the Fimmvörðuháls Pass (see Table 1). Even in this case, micro-earthquake locations corroborate the assumption that the second event of interaction took place between 6.5 and 4.5 km of depth and that this final event of magma mixing was the triggering mechanism for the intrusion of an E-W-oriented dike from the shallow storage zone up to the Fimmvörðuháls Pass (Fig. 7; cf. Tarasewicz et al. 2012).

Considering that the distance covered by the intruding magma between the sites of the two mixing processes is ~17 km and that the obtained timescales for the two mixing events are ~30 and ~15 days, respectively, the calculated average magma ascent rate is in the order of 0.01 m/s. These ascent rates refer to magma migration in the deep levels of the Eyjafjallajökull plumbing system, and are well in the range expected for basaltic liquids (e.g., Rutherford 2008, and references therein; Armienti et al. 2013). Evaluation of the ascent rate at shallow levels is more complex due to the influence of several variables (i.e., gas exsolution, conduit dynamics, fracture opening, etc.). In this regard, literature data for other basaltic volcanoes indicate extrusive ascent rates, especially for the early explosive phase of the eruption, up to one order of magnitude higher than those derived for migration in the deep levels of the plumbing system (cf. Rutherford 2008, and references therein).

Implications

The Fe-Mg diffusion modeling in olivine chemical profiles found in products of the 2010 eruption at the Fimmvörðuháls Pass (Eyjafjallajökull volcano, Iceland) have been used to reconstruct

the pre-eruptive history of the emitted magmas. Our approach has led to the comprehension of the dynamics of magmatic processes and of their timescales prior to the eruption. All the data available support the idea of a multilevel storage system beneath the Eyjafjallajökull volcano, where a poorly evolved magma ascending to the surface experienced multiple events of mixing with other magmas slightly different in their evolutionary degree. The equilibration through diffusion in three olivine populations, as a consequence of the interactions, constrains the timescales of transfer dynamics from the deep levels of the plumbing system (21–24 km of depth) toward the shallow reservoirs (4.5–6.5 km of depth) at ascent rates estimated at 0.01 m/s. Our study elucidates the physical configuration of volcanic systems grown in ocean ridge settings, emphasizing the possibility that magmas undergo complex processes during their storage and transport in the crust. Since the evidence of the first intrusion, the magma upraises from deep levels of the feeding system to the surface in a short timespan; this means that injection of primitive magmas in the deep reservoirs can trigger significant eruptions in short times.

Acknowledgments

Fieldwork and the analytical results presented in this study have been made possible through financial support from the University of Catania (Italy) to Marco Viccaro. Comments, suggestions, and corrections provided by the Associate Editor G. Zellmer, and the reviewers Corliss K.I. Sio and Christy B. Till helped to improve quality and clarity of this paper.

References cited

Armienti, P., Perinelli, C., and Putirka, K.D. (2013) A new model to estimate deep-level magma ascent rates, with applications to Mt. Etna (Sicily, Italy). Journal of Petrology, 54, 795–813.

Asimov, P.D., and Ghiorso, M.S. (1998) Algorithmic modifications extending MELTS to 500 calculate subsolidus phase relations. American Mineralogist, 83, 1127–1131.

Costa, F., and Chakraborty, S. (2004) Decadal time gap between mafic intrusion and silicic eruption obtained from chemical zoning patterns in olivine. Earth and Planetary Science Letters, 227, 517–530.

Costa, F., and Morgan, D.J. (2010) Time constraints from chemical equilibration in magmatic crystals. In A. Dosseto, S.P. Turner, and J.A. Van Orman, Eds., Timescales of Magmatic Processes: From Core to Atmosphere, p. 125–159. Wiley-Blackwell, U.K.

Costa, F., Chakraborty, S., and Dohmen, R. (2003) Diffusion coupling between trace and major elements and a model for calculation of magma residence times using plagioclase. Geochimica et Cosmochimica Acta, 67, 2189–2200.

Costa, F., Dohmen, R., and Chakraborty, S. (2008) Timescales of magmatic processes from modeling the zoning patterns of crystals. In K.D. Putirka and F.J. Tepley III, Eds., Minerals, Inclusions and Volcanic Processes, 69, 545–594. Reviews in Mineralogy and Geochemistry, Mineralogical Society of America, Chantilly, Virginia.

Dohmen, R., and Chakraborty, S. (2007) Fe-Mg diffusion in olivine II: point defect chemistry, change of diffusion mechanisms and a model for calculation of diffusion coefficients in natural olivine. Physics and Chemistry of Minerals, 34, 597–598.

Dugmore, A.J., Newton, A.J., Smith, K.T., and Mairs, K.A. (2013) Tephrochronology and the late Holocene volcanic and flood history of Eyjafjallajökull, Iceland. Journal of Quaternary Science, 28, 237–247.

Dunn, R.A., Toomey, D.R., and Solomon, S.C. (2000) Three-dimensional seismic structure and physical properties of the crust and shallow mantle beneath the East Pacific Rise at 9 degrees 30′N. Journal of Geophysical Research—Solid Earth, 105, B, 10, 23537–23555.

Ghiorso, M.S., and Sack, R.O. (1995) Chemical mass transfer in magmatic processes 4. A revised and internally consistent thermodynamic model for the interpolation and extrapolation of liquid-solid equilibria in magmatic systems at elevated temperatures. Contributions to Mineralogy and Petrology, 119, 197–212.

Ginibre, C., Woerner, G., and Kronz, A. (2007) Crystal zoning as an archive for magma evolution. Elements, 3, 261–266.

Gudmundsson, M.T., Pedersen, R., Vogfjörd, K., Thorbjarnardóttir, B., Jakobsdóttir, S., and Roberts, M.J. (2010) Eruptions of Eyjafjallajökull Volcano, Iceland. Eos, 91, p. 191.

Herzberg, C., and O'Hara, M.J. (1998) Phase equilibrium constraints on the origin of basalts, picrites, and komatiites. Earth-Science Reviews, 44, 39–79.

Kahl, M., Chakraborty, S., Costa, F., and Pompilio, M. (2011) Dynamic plumbing system beneath volcanoes revealed by kinetic modeling and the connection to monitoring data: an example from Mt. Etna. Earth and Planetary Science Letters, 308, 11–22.

Kahl, M., Chakraborty, S., Costa, F., Pompilio, M., Liuzzo, M., and Viccaro, M. (2013) Compositionally zoned crystals and real-time degassing data reveal changes in magma transfer dynamics during the 2006 summit eruptive episodes of Mt. Etna. Bulletin of Volcanology, 75, 692.

Keiding, J.K., and Sigmarsson, O. (2012) Geothermobarometry of the 2010 Eyjafjallajökull eruption: New constraints on Icelandic magma plumbing systems. Journal of Geophysical Research—Solid Earth, 117, B00C09.

Morgan, D.J., and Blake, S. (2006) Magmatic residence times of zoned phenocrysts: introduction and application of the binary element diffusion modelling (BEDM) technique. Contributions to Mineralogy and Petrology, 151, 58–70.

Morgan, D.J., Blake, S., Rogers, N.W., De Vivo, B., Rolandi, G., Macdonald, R., and Hawkesworth, C.J. (2004) Timescales of crystal residence and magma chamber volume from modelling of diffusion profiles in phenocrysts: Vesuvius 1944. Earth and Planetary Science Letters, 222, 933–946.

Moune, S., Sigmarsson, O., Schiano, P., Thordarson, T., and Keiding, J. K. (2012) Melt inclusion constraints on the magma source of Eyjafjallajökull 2010 flank eruption. Journal of Geophysical Research—Solid Earth, 117, B00C07.

Pedersen, R., and Sigmundsson, F. (2004) InSAR based sill model links spatially offset areas of deformation and seismicity for the 1994 unrest episode at Eyjafjallajökull volcano, Iceland. Geophysical Research Letters, 31, L14610.

——— (2006) Temporal development of the 1999 intrusive episode in the Eyjafjallajökull volcano, Iceland, derived from InSAR images. Bulletin of Volcanology, 68, 377–393.

Putirka, K.D. (2005) Igneous thermometers and barometers based on plagioclase plus liquid equilibria: Tests of some existing models and new calibrations. American Mineralogist, 99, 336–346.

Roeder, P.L., and Emslie, R.F. (1970) Olivine-liquid equilibrium. Contributions to Mineralogy and Petrology, 29, 275–289.

Rutherford, M.J. (2008) Magma ascent rates. In K.D. Putirka and F.J. Tepley III, Eds., Minerals, Inclusions and Volcanic Processes, 69, p. 241–271. Reviews in Mineralogy and Geochemistry, Mineralogical Society of America, Chantilly, Virginia.

Searle, R. (2013) Mid-Ocean Ridges. Cambridge University Press, 330 pp.

Shea, T., Costa, F., Krimer, D., and Hammer, J.E. (2015) Accuracy of timescales retrieved from diffusion modeling in olivine: a 3D perspective. American Mineralogist, 10, 2026–2042.

Sigmarsson, O., Vlastelic, I., Andreasen, R., Bindeman, I., Devidal, J.L., Moune, S., Keiding, J.K., Larsen, G., Hoskuldsson, A., and Thordarson, T. (2011) Remobilization of silicic intrusion by mafic magmas during the 2010 Eyjafjallajökull eruption. Solid Earth, 2, 271–281.

Sigmundsson, F., Hreinsdottir, S., Hooper, A., Arnadottir, T., Pedersen, R., Roberts, M.J., Oskarsson, N., Auriac, A., Decriem, J., Einarsson, P., Geirsson, H., Hensch, M., Ofeigsson, B.G., Sturkell, E., Sveinbjornsson, H., and Feigl, K.L. (2010) Intrusion triggering of the 2010 Eyjafjallajökull explosive eruption. Nature, 468, 426–430.

Streck, M.J. (2008) Mineral textures and zoning as evidence for open system processes. In K.D. Putirka and F.J. Tepley III, Eds., Minerals, Inclusions and Volcanic Processes, 69, p. 595–622. Reviews in Mineralogy and Geochemistry, Mineralogical Society of America, Chantilly, Virginia.

Sturkell, E., Sigmundsson, F., and Einarsson, P. (2003) Recent unrest and magma movements at Eyjafjallajökull and Katla volcanoes, Iceland. Journal of Geophysical Research—Solid Earth, 108, B, 8, 2369.

Tarasewicz, J., Brandsdottir, B., White, R. S., Hensch, M., and Bergthora, T. (2012) Using microearthquakes to track repeated magma intrusions beneath the Eyjafjallajökull stratovolcano, Iceland. Journal of Geophysical Research—Solid Earth, 117, B00C06.

Thordarson, T., and Larsen, G. (2007) Volcanism in Iceland in historical time: Volcano types, eruption styles and eruptive history. Conference: Penrose Conference on Beyond the Plume Hypothesis, Tests of the Plume Paradigm and Alternatives Location: Hverageroi, Iceland, AUG 25-29. Journal of Geodynamics, 43, 118–152.

Toplis, M.J. (2005) The thermodynamics of iron and magnesium partitioning between olivine and liquid: criteria for assessing and predicting equilibrium in natural and experimental systems. Contributions to Mineralogy and Petrology, 149, 22–39.

Viccaro, M., Giacomoni, P.P., Ferlito, C., and Cristofolini, R. (2010) Dynamics of magma supply at Mt. Etna volcano (Southern Italy) as revealed by textural and compositional features of plagioclase phenocrysts. Lithos, 116, 77–91.

Wallace, G.S., and Bergantz, G.W. (2002) Wavelet-based correlation (WBC) of zoned crystal populations and magma mixing. Earth and Planetary Science Letters, 202, 133–145.

——— (2004) Constraints on mingling of crystal populations from off-center zoning profiles: A statistical approach. American Mineralogist, 89, 64–73.

——— (2005) Reconciling heterogeneity in crystal zoning data: An application of shared characteristic diagrams at Chaos Crags, Lassen Volcanic Center, California. Contributions to Mineralogy and Petrology, 149, 98–112.

Zellmer, J.F., Blake, S., Vance, D., Hawkesworth, C., and Turner, S. (1999) Plagioclase residence times at two island arc volcanoes (Kameni Islands, Santorini, and Soufriere, St. Vincent) determined by Sr diffusion systematics. Contributions to Mineralogy and Petrology, 136, 345–357.

Manuscript received March 27, 2015
Manuscript accepted July 14, 2015
Manuscript handled by Georg Zellmer